


RESEARCH ARTICLE

Biomechanical Study of Intramedullary *Versus* Extramedullary Implants for Four Types of Subtrochanteric Femoral Fracture

Jie Wang, MD¹, Haobo Jia, MD¹, Xinlong Ma, MD^{1,2} , Jianxiong Ma, MD², Bin Lu, MD², Haohao Bai, MD², Ying Wang, MD²

Department of ¹Orthopaedics and ²Orthopaedics Institute, Tianjin Hospital, Tianjin, China

Objectives: To compare the biomechanical performance of proximal femoral nail anti-rotation (PFNA), the “upside-down” less invasive plating system (LISS), and proximal femoral locking plate (PFLP) in fixing different fracture models of subtrochanteric fractures.

Methods: Thirty composite femurs were divided into three equal groups (PFNA, PFLP, and reverse LISS). The implant-femur constructs were tested under axial compression load (0–1400 N) from models I to IV, which represented the Seinsheimer type I subtrochanteric fracture, type IIIa subtrochanteric fracture with the posteromedial fragment reduced; type IIIa subtrochanteric fracture with the posteromedial fragment lost; and type IV subtrochanteric fracture, respectively. Axial stiffness was analyzed for each group. Each group was then divided into two subgroups, one of which underwent torsional and axial compression failure testing, while the other subgroup underwent axial compression fatigue testing. The torsional stiffness, failure load, and cycles to failure were analyzed.

Results: PFNA had the highest axial stiffness ($F = 761.265$, $p < 0.0001$) and failure load ($F = 48.801$, $p < 0.0001$) in model IV. The axial stiffness and failure load of the PFLP were significantly higher than those of the LISS ($p < 0.0001$, $p = 0.001$). However, no significant difference in axial stiffness was found between models I to III (model I: $F = 2.439$, $p = 0.106$; model II: $F = 2.745$, $p = 0.082$; model III: $F = 0.852$, $p = 0.438$) or torsional stiffness in model IV ($F = 1.784$, $p = 0.187$). In fatigue testing, PFNA did not suffer from construct failure after 90,000 cycles of axial compression. PFLP and LISS were damaged within 14,000 cycles, although LISS withstood more cycles than PFLP ($t = 3.328$, $p = 0.01$).

Conclusion: The axial stiffness of the three implants was similar in models I to III. The biomechanical properties of PFNA were the best of the three implants in terms of axial stiffness, failure load, and fatigue testing cycles in model IV. The axial stiffness and failure load of the PFLP were better than those of the reverse LISS, but PFLP had fewer cycles in the fatigue tests than the reverse LISS.

Key words: Biomechanical; Extramedullary fixation; Fatigue test; Intramedullary nail; Subtrochanteric fractures

Introduction

Subtrochanteric fracture (STF) often occurs in people over 60 years old. Because of the high incidence of STF in older adults, early mobilization and prevention of the complications of long-term immobilization are important. The characteristics of the subtrochanteric region make these

fractures more demanding for the treating physician. There are high compressive stresses medially and high tensile stresses laterally¹, and deforming muscle forces make fracture reduction challenging. Moreover, the blood supply of the subtrochanteric region is more vulnerable². The high stresses, complicated deforming muscle forces, and decreased

Address for correspondence Jie Wang and Xinlong Ma, Department of Orthopedics, Tianjin Hospital, No. 406, Jiefang Nan Street, Hexi District, Tianjin, China. Email: wjz10885@163.com Xinlong Ma, Department of Orthopedics and Department of Orthopaedics Institute, Tianjin Hospital, No. 406, Jiefang Nan Street, Hexi District, Tianjin, China. Email: wangjie@tjmu.edu.cn

Jie Wang and Haobo Jia contributed equally to this study.

Received 2 March 2021; accepted 20 May 2022

TABLE 1 Design characteristics of the implants and the fixation constructs

| Implant | Implant type | Materials | Implant length (Hole/mm) | Proximal fixation (number, length and the others) | Shaft fixation (number, length and the others) |
|---------|---------------------|----------------|---------------------------|--|--|
| PFNA | Intramedullary nail | Titanium alloy | 3/200 mm (diameter 11 mm) | One 95-mm 10-mm anti-rotational blade | One 30-mm 4.9-mm bicortical screws |
| PFLP | Locking plate | Titanium alloy | 9/240 mm | One 65-mm, one 60-mm and one 76-mm 7.3-mm cannulated proximal locking screws | One 38-mm (hole 3) and three 36-mm (hole 5, 7, and 9) 5-mm bicortical locking screws |
| LISS | Locking plate | Titanium alloy | 9/230 mm | One 30-mm (95°), one 40-mm (120°), one 46-mm (135°), one 50-mm and one 56-mm 5.0-mm unicortical screws | One 38-mm (hole 3) and three 36-mm (hole 5, 7 and 9) 5-mm bicortical locking screws |

vascularity of the region have been associated with high levels of complications, including impaired fracture healing and implant failure, characterized by varus collapse of the fracture³.

The selection of implants for the surgical management of STFs is difficult. Furthermore, different types of STFs may require different implants. Many randomized controlled trials^{3,4} have reported different findings in this area. To date, many types of implants for the fixation of STF have been developed. The proximal femoral nail anti-rotation (PFNA) was designed to provide rotational and angular stability with one femoral neck helically shaped blade by compaction of cancellous bone around the blade during insertion⁵, which increases resistance to cutout⁶. The less invasive plating system (LISS) was designed to treat distal femoral fractures with minimally invasive surgery. A few biomechanical studies have compared LISS with other implants for the treatment of STF. The proximal femoral locking plate (PFLP) allows limited-contact and angular-stable plating for the treatment of peritrochanteric fractures^{7,8}. The angles of the three proximal locking holes are 95°, 120°, and 135°, which allow multiple angular-stable fixation points into the proximal femur with cannulated or cancellous screws, while the remaining distal holes were designed to obtain shaft fixation with locking or non-locking cortex screws.

It remains unclear whether intramedullary fixation or extramedullary fixation is better for different types of STF. Moreover, it is unclear whether the medial buttress of the STF is important for the stability of fixing the fracture. Therefore, this study aimed to (i) evaluate the differences in axial stiffness, torsional stiffness, and axial failure load of PFNA, reverse LISS, and PFLP for fixing different types of STF; (ii) evaluate the differences in cycles to failure among the three implants; and (iii) analyze the importance of medial buttress to the stability of fixing the STF.

Materials and Methods

Specimen Preparation

A total of 30 fourth-generation synthetic composite left adult femurs (Sawbones; Model 3403, Pacific Research Labs Inc., Vashon, WA) with 11-mm diameter intramedullary canals were obtained and randomly divided into three groups

($n = 10$ for each group) for fixation with PFNA, LISS, or PFLP. The configurations of the three implants are listed in Table 1. The fractured composite femurs were fixed according to the manufacturer's guidelines by the same surgeon. Then, the implant-femur constructs were tested using X-rays to ensure that the optimal implant position was achieved (Figure 1). Each of the implant-femur constructs was tested in four fracture models: (i) Model I: Each femur was sawn transversely 3 cm distal to the apex of the lesser trochanter to simulate an AO/OTA 32A3 fracture; (ii) Model II: Medial wedge osteotomy was performed on the same implant-femur construct at the proximal end of the distal fracture fragment within a 2 cm region to simulate an AO/OTA 32B2 fracture. One #18 stainless steel wire was used to strap the wedge fragment remaining in the normal position; (iii) Model III: The wedge fragment was removed from Model II; (iv) Model IV: The bone remaining within the region from 3 cm to 5 cm distal to the apex of the lesser trochanter was removed to simulate an AO/OTA 32C3

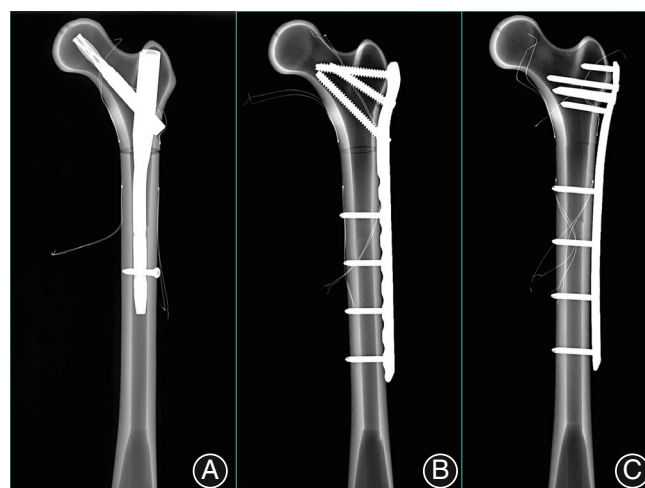


Fig. 1 Radiographs of three exemplified implant-femur constructs. (A) PFNA; (B) PFLP; (C) LISS. All implants were fixed by one surgeon according to the manufacturer's guidelines. The X-rays show that the position of each implant in the femur was good

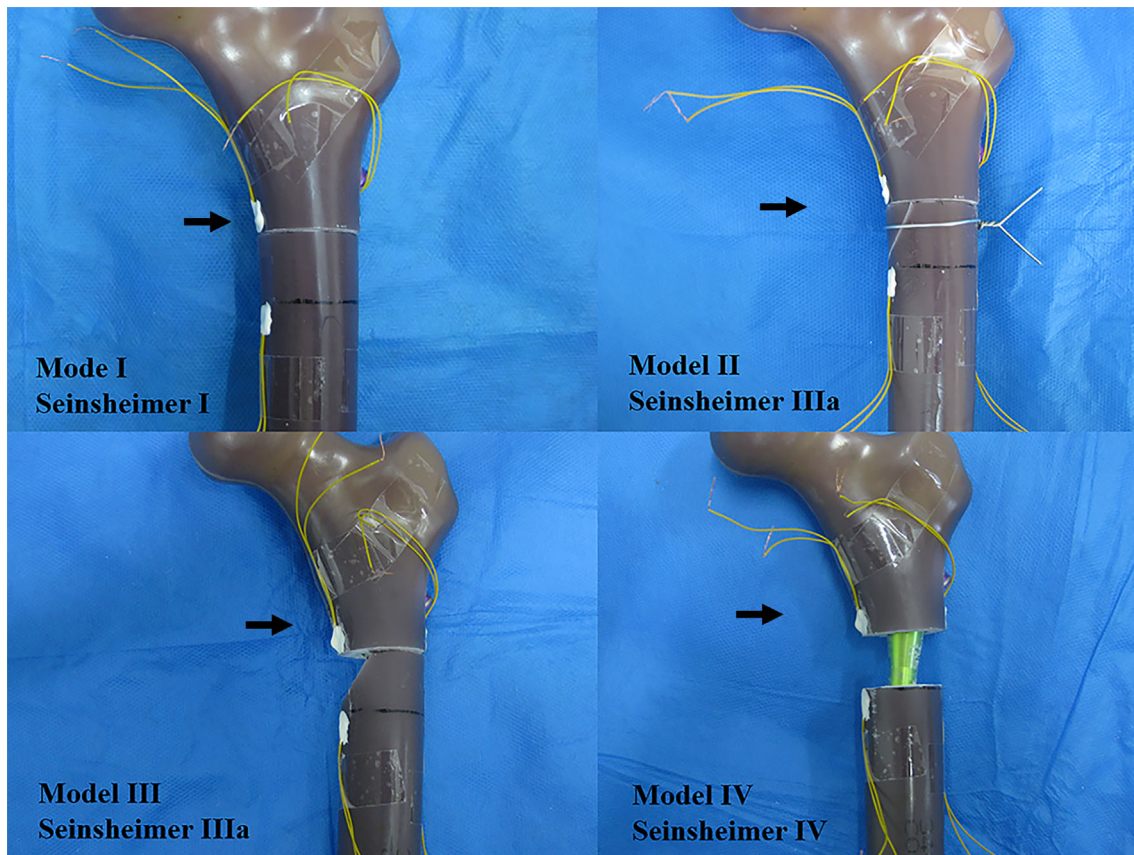


Fig. 2 Photos of a specimen representing the four fracture models for testing (black arrows indicate the characteristics of different fracture types). (A) Model I: Seinsheimer type I subtrochanteric fracture; (B) Model II: Seinsheimer type IIIa subtrochanteric fracture with the posteromedial fragment reduced; (C) Seinsheimer type IIIa subtrochanteric fracture with the posteromedial fragment lost; (D) Seinsheimer type IV subtrochanteric fracture

fracture (Figure 2). The fracture model of each implant-femur construct was subsequently created and tested following testing of the previous fracture model. The implant was not removed during the testing.

Biomechanical Testing

The distal end of the implant-femur construct was potted in a metal tube at 6° valgus in the frontal plane and vertical in the sagittal plane to simulate anatomic positioning⁹, using polymethylmethacrylate. A custom cup simulating the acetabulum was used to secure the femoral head, which allowed the femoral head to rotate within the cup. The constraint method was similar to that used by Forward *et al.*¹⁰ (Figure 3), and the whole unit was attached to the testing machine (Bose ElectroForce 3510 Test Instrument, New Castle, USA).

Each implant-femur construct was preloaded and maintained at 500 N for 30 s before testing to consolidate all constructs equally, ensuring that all the cortical surfaces were mated, and no spurious displacements occurred before testing. The following four loading protocols were applied to the implant-femur constructs (Figure 4):

- i. An axial compression test was performed on each implant-femur construct from models I to IV. After preloading, axial loading was added to the implant-femur construct at a velocity of 10 mm/min from 0 to 1400 N (approximately twice the bodyweight of 70 kg).
- ii. A torsional test was performed on model IV only. After axial compression testing on model IV, the implant-femur constructs were all preloaded and maintained at 2 Nm of torque for 30 s to remove any slack in the system, using a custom jig to clamp the proximal part of the femur (Figure 3). After preloading, the implant-femur constructs were loaded at a rate of 0.05 rad/s up to 10 Nm of torque.
- iii. An axial compression failure test was performed on model IV. After axial and torsional testing, the implant-femur constructs in each implant group were randomly divided into two subgroups ($n = 5$ for each subgroup). Five implant-femur constructs in each implant group were axially loaded to failure from 0 N at a velocity of 10 mm/min.
- iv. A cyclic axial compression fatigue loading test was performed on model IV. Another five implant-femur

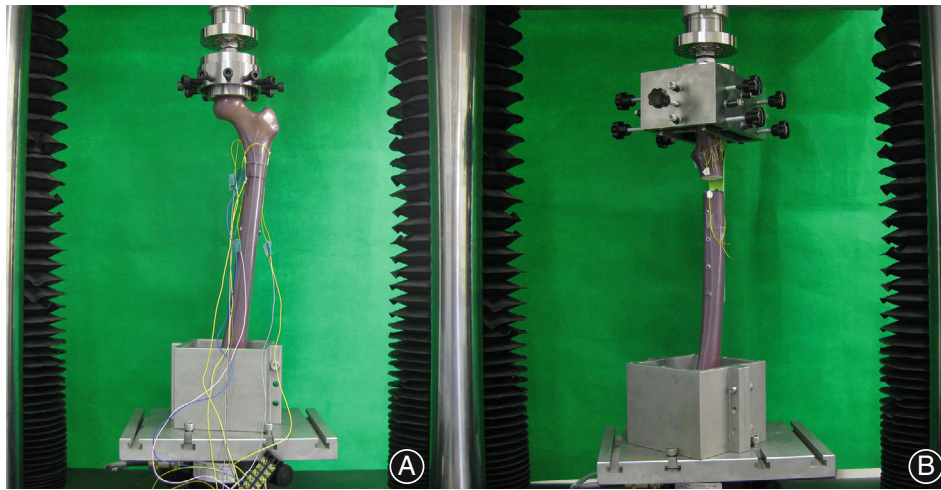


Fig. 3 Loading apparatus with the implant-femur construct on it. (A) Axial compression test. The load was applied along the mechanical axis. The distal end of the implant-femur construct was potted in a metal tube at 6° valgus in the frontal plane and vertical in the sagittal plane to simulate anatomic positioning, using polymethylmethacrylate. A polymethylmethacrylate custom cup simulating the acetabulum was used to secure the femoral head, and it was attached to the machine actuator by a custom jig; (B) Torsional test. The rotation axis was the mechanical axis. The position of the femur was the same as that in the axial test. The proximal part of the femur was clamped by a custom jig, bearing the anterior and posterior sides against the plates and permitting resistance to torsional moments

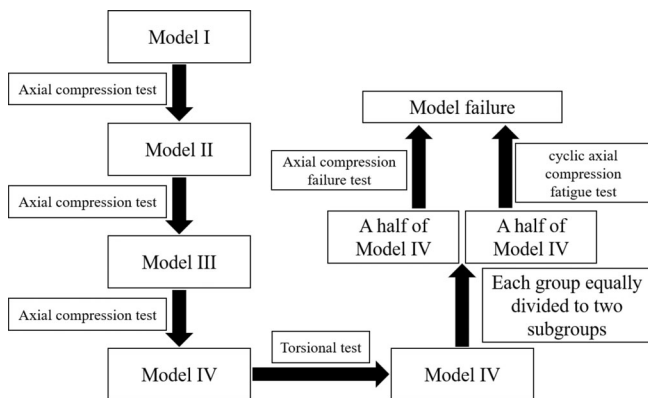


Fig. 4 A flow chart of the model making and mechanical tests

constructs in each implant group were loaded from 140 N to 1400 N in a sinusoidal manner at 3 Hz until 90,000 cycles¹¹, or until one of the construct failure criteria was met.

In testing forms (iii) and (iv), these conditions were defined as construct failure: fracture of the femur or implant, screw penetrating the femoral head or neck, varus plastic deformation of the implant, or 20-mm femoral head axial displacement. The failure load and modes of failure in testing form (iii), cycles to failure, and modes of fatigue failure in testing form (iv) were recorded. Machine data in terms of displacement, angle, cycles, and load were recorded during biomechanical testing at a rate of 20 Hz from the machine controller. For the axial and torsional testing, a load-

displacement curve and load-angle curve were plotted for each implant-femur construct, and axial or torsional stiffness was calculated as the slope of the linear portion of the curve.

Data Acquisition and Analysis

Data were first checked for normality of distribution before the application of parametric statistics. Data were analyzed using a one-way analysis of variance. Tukey's *post hoc* test was applied in any case in which the analysis of differences demonstrated significance under homogeneity of variance. Tamhane's T2 test was used as a follow-up when homogeneity of variance was not achieved. Statistical significance was set at $p < 0.05$. All statistical analyses were computed using SPSS version 11.0 (SPSS, Inc., Chicago, IL, USA).

Results

Axial and Torsional Stiffness

In terms of axial stiffness, there were no differences among the three implant-femur constructs in models I to III (model I: $F = 2.439$, $p = 0.106$; model II: $F = 2.745$, $p = 0.082$; model III: $F = 0.852$, $p = 0.438$). In model IV, differences were detected among the three implant-femur constructs ($F = 761.265$, $p < 0.0001$) for axial stiffness. Tukey's *post hoc* analysis showed that the PFNA construct was stiffer than the other two implant-femur constructs ($p < 0.0001$) and that the PFLP construct was stiffer than the LISS construct ($p < 0.0001$) (Table 2).

There was no significant difference in axial stiffness between models II and III of the PFNA construct ($p = 0.170$), and there was a significant decrease in axial

TABLE 2 Axial and torsional stiffness of the implant-femur constructs in the four fracture models

| Implants | n | Axial stiffness (N/mm) | | | | Torsional stiffness (Nm/degree) |
|----------|----|------------------------|----------------|---------------|---------------------------|---------------------------------|
| | | Model I | Model II | Model III | Model IV | |
| PFNA | 10 | 1191.4 ± 204.9 | 985.6 ± 179.0 | 797.8 ± 178.9 | 352.7 ± 19.1 ^a | 1.97 ± 0.37 |
| PFLP | 10 | 1274.7 ± 207.4 | 1038.2 ± 180.3 | 741.8 ± 181.4 | 134.4 ± 12.5 ^b | 1.71 ± 0.55 |
| LISS | 10 | 1410.0 ± 254.3 | 1189.2 ± 239.9 | 856.4 ± 225.2 | 89.1 ± 16.2 | 2.11 ± 0.49 |
| F value | — | 2.439 | 2.745 | 0.852 | 761.265 | 1.784 |
| p value | — | 0.106 | 0.082 | 0.438 | < 0.0001 | 0.187 |

Note: Values are expressed as mean ± SD.; Note: F value: F value of one-way analysis of variance.; Note: p value: Results of one-way analysis of variance of each type of model.; ^a Significantly different from PFLP ($p < 0.0001$) and LISS ($p < 0.0001$); ^b Significantly different from LISS ($p < 0.0001$).

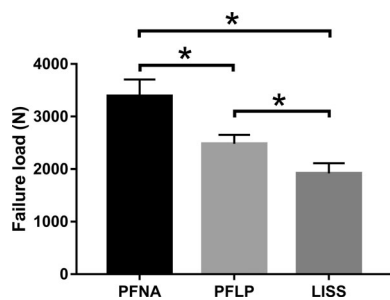


Fig. 5 Failure load of each implant-femur construct in axial compression failure tests. * indicates that a significant difference was detected between the two implant-femur constructs ($p < 0.05$)

stiffness between models II and III of the LISS ($p = 0.030$) and PFLP ($P = 0.011$) constructs, respectively (Table 2).

There were no significant differences among the three implant-femur constructs for torsional stiffness ($F = 1.784$, $p = 0.187$) (Table 2).

Failure Load and Modes of Failure

Differences were detected among the three implant-femur constructs ($n = 5$, $F = 48.801$, $p < 0.0001$) for the failure load. The PFNA construct withstood the highest failure load (3387.3 ± 316.6 N), greater than those of the plate constructs: 2483.3 ± 169.3 N ($n = 5$, $p < 0.0001$) for the PFLP construct, and 1917.7 ± 194.8 N ($n = 5$, $p < 0.0001$) for the LISS construct in axial compression failure test (Figure 5). The failure load of the PFLP construct was significantly higher than that of the LISS construct in the axial compression failure test ($n = 5$, $p = 0.007$) (Figure 5). The mode of failure of the five PFNA constructs was varus plastic deformation at the valgus junction of the PFNA (Figure 6(A)). The mode of failure of the five PFLP constructs and LISS constructs was a 20-mm femoral head axial displacement.

Cycles to Failure and Modes of Fatigue Failure

All five PFNA constructs withstood 90,000 cycles of axial compression loading, and no catastrophic failure occurred. The PFLP construct withstood $11,091 \pm 1533$ cycles ($n = 5$),



Fig. 6 Failure modes of the implants. (A): Failure mode of PFNA in the axial compression failure testing. The main nail of the PFNA was curved at the proximal part; (B): Failure mode of PFLP in fatigue testing. PFLP constructs a fracture at the level of the fourth screw hole of the plate; (C): Failure mode of LISS in fatigue testing. A fatigue crack emerged at the hole at the fracture site

which was less than the LISS construct at 13809 ± 993 cycles ($t = 3.328$, $p = 0.01$, $n = 5$, two-tailed t -test). The mode of fatigue failure of the five PFLP constructs was a fracture at the level of the fourth screw hole of the plate (Figure 6(B)). The mode of fatigue failure of the five LISS constructs was fatigue cracks at the hole along the fracture site (Figure 6(C)).

Discussion

The Axial Stiffness, Torsional Stiffness, and Axial Failure Load

As evidenced by our testing, there were no significant differences among the three constructs in terms of axial stiffness in models I, II, and III. Many biomechanical studies have not tested stable STFs. Our study is the first to explore the biomechanical properties of implants in fixing a stable STF. The implants were bent under axial loading, which led to mutual extrusion of the medial sides of the two fragments. However, there was axial and shear displacement at the fracture site^{12,13}. Moreover, the intramedullary nail had more shear displacement than the side plate¹². The main nail above the isthmus of the femoral shaft was likely to bend during axial loading. Part of the axial force was changed to a shear force during the bending of the nail. In plate fixing, the plate was fixed with the femoral shaft using several bicortical screws, which were more rigid than one locking screw in the PFNA.

There was no significant difference in axial stiffness between models II and III for the PFNA construct, but there was a significant decrease in axial stiffness between models II and III of the LISS and PFLP constructs. This indicates that posteromedial support is important for plate fixation. Wieser and Babst¹⁴ reported four cases of PFLP fixation failure, and their findings indicated that if medial cortical support is inadequate, osteosynthesis is subjected to severe bending stress, and the loads applied concentrate on the junction of the PFLP and the proximal locking screws.

In model IV, our results showed that the PFNA construct had the highest axial stiffness, failed at a significantly greater load in axial compression failure tests, and withstood significantly more cycles in the fatigue tests. This confirms that intramedullary devices have advantages over extramedullary fixation in the treatment of STF when a large gap is present. The biomechanical advantages of the intramedullary device are its central position and reduced lever arm for bending forces compared with the position of the plate on the lateral cortex. This may be of particular importance for fractures in which the medial-posterior buttress cannot be restored, or the subtrochanteric region has been completely comminuted. Previous biomechanical studies have demonstrated that intramedullary nails are biomechanically superior to locking plates^{9,10,15-19}. Clinical studies have reported that PFNA offers shorter times for fracture healing and weight-bearing^{20,21}, shorter radiation times, and better

Harris hip scores than reverse LISS and PFLP in the treatment of STF.

To the best of our knowledge, few biomechanical studies have reported on torsional stiffness^{19,22}. Our results show no difference in torsional stiffness among the three implant-femur constructs. This is in line with the study by Crist *et al.*²² in which no difference was detected among the plate-femur constructs. However, our results were different from those of Tencer *et al.*¹⁹, who found that the torsional stiffness of the intramedullary nail was less than that of the plate. Nevertheless, further biomechanical studies are required.

Cycles to Failure Among the Three Implants

The axial stiffness and failure load of the LISS construct were significantly lower than those of the PFLP construct in model IV. However, the LISS construct had significantly more cycles in the fatigue test in model IV than in the PFLP construct. The PFLP proximal triangle construct was more stable than the LISS, and the PFLP side plate was thicker than the LISS. These two factors might explain the higher axial stiffness and failure load of the PFLP. However, the triangular construct produces a severe concentration of stress on the screw hole of the 135° locking screw, which might lead to fewer cycles for PFLP in the fatigue test and the complete breakage of PFLP in that region.

The Importance of Medial Buttress

With the popularization and application of intramedullary and extramedullary fixations for the treatment of STF, there were many negative reports of intramedullary nails and extramedullary plate. The main complications were varus collapse and internal fixation failure, which eventually led to nonunion of fractures^{14,23-25}. The incidence of varus collapse in intramedullary fixation was about 23%, and the incidence of this complication in extramedullary fixation was 6% - 32%^{23,26}. Furthermore, studies showed that correction of varus malformation of fracture during operation and retention of medial cortical support were important factors in preventing nonunion of the fractures²³. Clinical studies also showed that the absence of medial or posteromedial cortical support led to failure and varus collapse in the intramedullary^{23,24} and extramedullary fixation^{14,27}. In our study, there was a significant decrease in axial stiffness between models II and III of the LISS and PFLP constructs. This was similar to the above clinical studies^{14,27}. However, there was no significant difference in axial stiffness between models II and III for the PFNA construct, which was different from the above clinical studies^{23,24}. Therefore, more clinical and biomechanical studies were needed to improve the evidence.

Limitation

Our study has several limitations. First, we used synthetic femurs; hence, our findings cannot be generalized to *in vivo* biomechanical properties. However, inter-specimen variability was lower than that for fresh frozen femurs, and the uniform dimensions of the composite femur allowed the same size

implants to be inserted in all specimens using the same technique. Composite femurs have been used successfully in previous mechanical testing of femoral implants²⁸. Second, our loading protocol might not accurately model the magnitude, direction, or number of loading cycles experienced physiologically. Further studies could test implant-femur constructs under normal gait conditions. Third, we did not assess the healing tissue or its stiffness and role during the healing process. Many researchers have used other methods (including external fixators²⁹ and finite element analysis³⁰) to assess fracture stiffness in healing calluses, which can be divided into soft and hard calluses with different properties. It is difficult to use appropriate substitutes to simulate calluses *in vitro*. However, further studies could simulate healing calluses using the three-dimensional finite element method.

Conclusion

As evidenced by our testing, the axial stiffness of the three implants was not significantly different among the implant-femur constructs in models I to III. The medial buttress of the subtrochanteric region is important for maintaining the stability of the STF fixed with PFLP or LISS. The biomechanical properties of PFNA were the best of the three implants in terms of axial stiffness, failure load, and fatigue testing cycles in model IV. The axial stiffness and failure load of the PFLP were better than those of the reverse LISS, but PFLP had fewer cycles in the fatigue tests than the

reverse LISS. No difference in torsional stiffness was detected among the three implants.

Authors' Contributions

Jie Wang and Haobo Jia conceived and designed this study; Jianxiong Ma and Bin Lu perform the biomechanical test; Haohao Bai and Ying Wang performed the statistical analysis; Xinlong Ma provided clinical guidance. All authors critically revised the manuscript.

Authorship Declaration

All authors listed meet the authorship criteria according to the latest guidelines of the International Committee of Medical Journal Editors, and all authors are in agreement with the manuscript.

Acknowledgements

This work has received specific grant funding from the National Natural Science Foundation of China (81601893), the Tianjin Natural Science Foundation (17JQJNC10900), and the Tianjin Enterprise Postdoctoral Innovation Project (TJQYBSH2017013).

Conflict of Interest Statement

All named authors hereby declare that they have no conflicts of interest to disclose.

References

- Koch JC. The laws of bone architecture. *Am J Anat.* 1917;21:177–298.
- de Toledo B, Lourenco PR, Pires RE. Subtrochanteric fractures of the femur: update. *Rev Bras Ortop.* 2016;51:246–53.
- Rahme DM, Harris IA. Intramedullary nailing versus fixed angle blade plating for subtrochanteric femoral fractures: a prospective randomised controlled trial. *J Orthop Surg.* 2007;15:278–81.
- Lee PC, Hsieh PH, Yu SW, Shiao CW, Kao HK, Wu CC. Biologic plating versus intramedullary nailing for comminuted subtrochanteric fractures in young adults: a prospective, randomized study of 66 cases. *J Dent Traumatol.* 2007;63:1283–91.
- Strauss E, Frank J, Lee J, Kummer FJ, Tejwani N. Helical blade versus sliding hip screw for treatment of unstable intertrochanteric hip fractures: a biomechanical evaluation. *Injury.* 2006;37:984–9.
- Sommers MB, Roth C, Hall H, Kam BCC, Ehmke LW, Krieg JC, et al. A laboratory model to evaluate cutout resistance of implants for peritrochanteric fracture fixation. *J Orthop Trauma.* 2004;18:361–8.
- Hasenboehler EA, Agudelo JF, Morgan SJ, Smith WR, Hak DJ, Stahel PF. Treatment of complex proximal femoral fractures with the proximal femur locking compression plate. *Orthopedics.* 2007;30:618–23.
- Zderic I, Oh JK, Stoffel K, Sommer C, Helfen T, Camino G, et al. Biomechanical analysis of the proximal femoral locking compression plate: do quality of reduction and screw orientation influence construct stability? *J Orthop Trauma.* 2018;32:67–74.
- Kim JW, Oh CW, Byun YS, Oh JK, Kim HJ, Min WK, et al. A biomechanical analysis of locking plate fixation with minimally invasive plate osteosynthesis in a subtrochanteric fracture model. *J Trauma.* 2011;70:E19–23.
- Forward DP, Doro CJ, O'Toole RV, Kim H, Floyd JCP, Sciadini MF, et al. A biomechanical comparison of a locking plate, a nail, and a 95 degrees angled blade plate for fixation of subtrochanteric femoral fractures. *J Orthop Trauma.* 2012;26:334–40.
- Schmalzried TP, Szuszczewicz ES, Northfield MR, et al. Quantitative assessment of walking activity after total hip or knee replacement. *J Bone Joint Surg Am.* 1998;80:54–9.
- Bredbenner TL, Snyder SA, Mazloomi FR, le T, Wilber RG. Subtrochanteric fixation stability depends on discrete fracture surface points. *Clin Orthop Relat Res.* 2005;432:217–25.
- Roberts CS, Nawab A, Wang M, voor MJ, Seligson D. Second generation intramedullary nailing of subtrochanteric femur fractures: a biomechanical study of fracture site motion. *J Orthop Trauma.* 2002;16:231–8.
- Wieser K, Babst R. Fixation failure of the LCP proximal femoral plate 4.5/5.0 in patients with missing posteromedial support in unstable per-, inter-, and subtrochanteric fractures of the proximal femur. *Arch Orthop Trauma Surg.* 2010;130:1281–7.
- Wang J, Ma JX, Jia HB, Chen Y, Yang Y, Ma XL. Biomechanical evaluation of four methods for internal fixation of comminuted subtrochanteric fractures. *Medicine.* 2016;95:e3382.
- Wang J, Ma XL, Ma JX, Xing D, Yang Y, Zhu SW, et al. Biomechanical analysis of four types of internal fixation in subtrochanteric fracture models. *Orthop Surg.* 2014;6:128–36.
- Curtis MJ, Jinnah RH, Wilson V, Cunningham BW. Proximal femoral fractures: a biomechanical study to compare intramedullary and extramedullary fixation. *Injury.* 1994;25:99–104.
- Ozkan K, Turkmen I, Sahin A, et al. A biomechanical comparison of proximal femoral nails and locking proximal anatomic femoral plates in femoral fracture fixation: a study on synthetic bones. *Indian J Orthop.* 2015;49:347–51.
- Tencer AF, Johnson KD, Johnston DW, et al. A biomechanical comparison of various methods of stabilization of subtrochanteric fractures of the femur. *J Orthop Res.* 1984;2:297–305.
- Han N, Sun GX, Li ZC, Li GF, Lu QY, Han QH, et al. Comparison of proximal femoral nail antirotation blade and reverse less invasive stabilization system-distal femur systems in the treatment of proximal femoral fractures. *Orthop Surg.* 2011;3:7–13.
- Imerci A, Canbek U, Karatosun V, et al. Nailing or plating for subtrochanteric femoral fractures: a non-randomized comparative study. *Eur J Orthop Surg Traumatol.* 2015, 2015;25:889–94.
- Crist BD, Khalafi A, Hazelwood SJ, Lee MA. A biomechanical comparison of locked plate fixation with percutaneous insertion capability versus the angled blade plate in a subtrochanteric fracture gap model. *J Orthop Trauma.* 2009;23:622–7.
- Krappingger D, Wolf B, Dammerer D, Thaler M, Schwendinger P, Lindtner RA. Risk factors for nonunion after intramedullary nailing of subtrochanteric femoral fractures. *Arch Orthop Trauma Surg.* 2019;139:769–77.

- 24.** Hao Y, Zhang Z, Zhou F, Ji H, Tian Y, Guo Y, et al. Risk factors for implant failure in reverseoblique and transverse intertrochanteric fractures treated with proximal femoral nail antirotation (PFNA). *J Orthop Surg Res.* 2019;14:350.
- 25.** Glassner PJ, Tejwani NC. Failure of proximal femoral locking compression plate: a case series. *J Orthop Trauma.* 2011;25:76–83.
- 26.** Shah MD, Kapoor CS, Soni RJ, Patwa JJ, Golwala PP. Evaluation of outcome of proximal femur locking compression plate (PFLCP) in unstable proximal femur fractures. *J Clin Orthop Trauma.* 2017;8:308–12.
- 27.** Streubel PN, Moustoukas MJ, Obremsky WT. Mechanical failure after locking plate fixation of unstable intertrochanteric femur fractures. *J Orthop Trauma.* 2013;27:22–8.
- 28.** Floyd JC, O'Toole RV, Stall A, et al. Biomechanical comparison of proximal locking plates and blade plates for the treatment of comminuted subtrochanteric femoral fractures. *J Orthop Trauma.* 2009;23:628–33.
- 29.** Richardson JB, Kenwright J, Cunningham JL. Fracture stiffness measurement in the assessment and management of tibial fractures. *Clin Biomech.* 1992;7: 75–9.
- 30.** Shefelbine SJ, Simon U, Claes L, Gold A, Gabet Y, Bab I, et al. Prediction of fracture callus mechanical properties using micro-CT images and voxel-based finite element analysis. *Bone.* 2005;36:480–8.